physica **pssb** status solidi

www.pss-b.com

basic solid state physics

Kinetics study of vacancy–oxygen-related defects in monocrystalline solar silicon

V. Quemener*,1, B. Raeissi1, F. Herklotz1, L. I. Murin1,2, E. V. Monakhov1, and B. G. Svensson1

1 University of Oslo, Department of Physics/Center for Materials Science and Nanotechnology,
  P.O. Box 1048 Blindern, N-0316 Oslo, Norway
2 Scientific-Practical Materials Research Center of NAS of Belarus, Minsk 220072, Belarus

─────────────
* Corresponding author: e-mail vincent.quemener@smn.uio.no, Phone: +47-22 84 09 44, Fax: +47-22 85 64 22

In this work, diffusion and dissociation mechanisms related to the formation and evolution of vacancy–oxygen complexes have been studied. Czochralski-grown silicon samples have been irradiated at room temperature using fast electrons resulting in the formation of several defects including vacancy–oxygen complexes (VO_n). The samples were isothermally annealed at different temperatures in the range of 370–470 °C. Fourier-transform infrared spectroscopy has been employed to measure the local vibrational modes associated with the individual defects. The evolution and generation kinetics of vacancy–oxygen complexes have been simulated within the framework of the theory for diffusion-limited reactions and compared with the experimental data.

© 2014 WILEY-VCH Verlag GmbH & Co. KGaA, Weinheim

1 Introduction Silicon is the most important semiconductor for photovoltaic applications. The need to improve the quality while keeping low production cost, demands a full understanding of impurities and intrinsic related defects in silicon. In particular, oxygen is one of the most important impurities in solar-grade silicon, and influences the major defects formed during silicon crystallization and high temperature processing. For instance, oxygen related defects are, presumably, responsible for the light-induced degradation effect, which dramatically decreases the efficiency of the photovoltaic cells [1]. Moreover, electrically active and inactive centers like oxygen complexes (O_n) and vacancy–oxygen complexes (VO_n) are the most frequently appearing defects (n is an integer ≥ 1) [2–5]. These defects play a central role in the formation of oxygen precipitates and thermal donors [6–9]. Thus, understanding of the diffusion and dissociation mechanisms associated with the formation and evolution of the VO_n defects is crucial to control their impact. One of the most successful methods for studying oxygen-containing defect centers in silicon is local vibrational mode (LVM) spectroscopy. In particular, Fourier-transform infrared spectroscopy (FTIR) has been used to identify oxygen dimers, trimers, and a number of vacancy-oxygen complexes. So far, VO and VO_2 centers have been extensively studied and some important information about their diffusion/dissociation mechanisms, especially for VO, has been obtained [9–11]. However, the evolution mechanism did not include larger VO_n cluster ($n = 3, 4$). Most recently, LVMs associated to VO_3 and VO_4 have been identified which enables investigations of their diffusion and dissociation properties in detail [4, 12, 13].

2 Experiments The samples used were cut from Cz-Si phosphorus doped wafers with concentrations of interstitial oxygen (O_i) and substitutional carbon (C_s) of $(1 - 1.3) \times 10^{18}$ cm^{-3} and $\leq 5 \times 10^{14}$ cm^{-3}, respectively. In order to increase the defect concentrations to readily detectable levels, the samples were irradiated with 2.5 MeV electrons at room temperature and fluences in the range of $(1 - 10) \times 10^{17}$ cm^{-2}. After irradiation, the samples were isothermally annealed in a tube furnace with nitrogen flow at 370, 400, 425, and 470 °C. After each annealing stage, the concentrations of O_i and VO_n defects were determined by FTIR. The measurements were performed using a Bruker IFS125 HR Fourier-transform IR spectrometer with the samples kept at room temperature and a spectral resolution of 1 cm^{-1}.
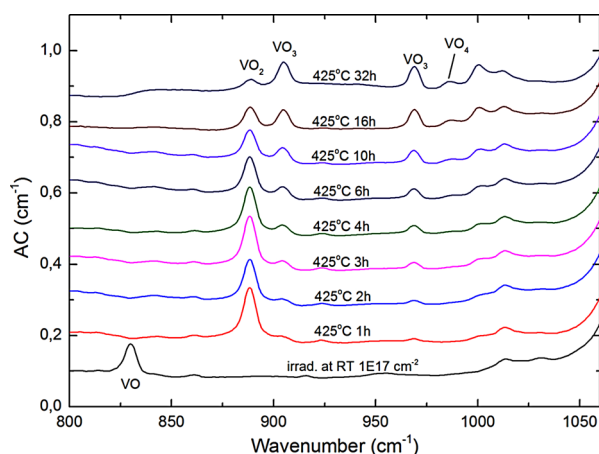
© 2014 WILEY-VCH Verlag GmbH & Co. KGaA, Weinheim

Figure 1 Section of absorption spectra measured at room temperature after irradiation and after isothermal annealing at 425 °C for different times up to 32 h.

Figure 2 Sum of the VO, VO_2, VO_3, and VO_4 species versus time during isothermal annealing at different temperatures.

The defect concentrations were monitored by measuring the peak intensities of the associated LVMs. For O_i (1107 cm^{-1}), VO (830 cm^{-1}), VO_2 (888.5 cm^{-1}), VO_3 (905, 969 cm^{-1}), and VO_4 (985 cm^{-1}), we used calibration coefficients of 3.14×10^{17}, 8.5×10^{16}, 4.25×10^{16}, 8.5×10^{16}, and 4.25×10^{16} cm^{-2}, respectively [13, 14].

3 Results and discussions Figure 1 shows absorption spectra of the sample isothermally annealed at 425 °C for different times. One can observe the vibrational bands related to VO, VO_2, VO_3 and VO_4, and their intensities change with the isothermal annealing duration. After irradiation, only VO is present, while upon annealing, a successive formation of VO_2, VO_3, and VO_4 occur. This can be described by a sequential formation of the different defects via the reaction:

$$VO_n + O_i \rightarrow VO_{n+1}, \quad (n \geq 1). \quad (1)$$
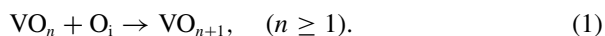
In order to describe the evolution of the defects and their concentrations, a model has been developed applying the theory of diffusion-limited reactions and assuming a sequential build-up of the vacancy-oxygen clusters, including diffusion/dissociation reactions [15]. A reaction occurs between two species when they migrate and agglomerate into a larger one after approaching each other within a capture radius R. The reaction rate is given by $4\pi R(D_A + D_B)[A][B]$, where D_A and D_B represent the diffusion constants and [A] and [B] are the concentrations of the two species A and B, respectively. In the present case, we used for the capture radius R a geometrical value of 5 Å. A back reaction occurs when a defect complex dissociates into smaller species. The dissociation is given by $K_C[C]$, where K_C represents the dissociation rate and [C] is the concentration of the species C. The diffusion and dissociation constants are described by the relations $D = d_0 \exp(-E_a/kT)$ and $K = k_0 \exp(-E_a/kT)$, respectively, where d_0 and k_0 are the prefactors, E_a is the activation energy, k is the Boltzmann constant and T is the absolute temperature.
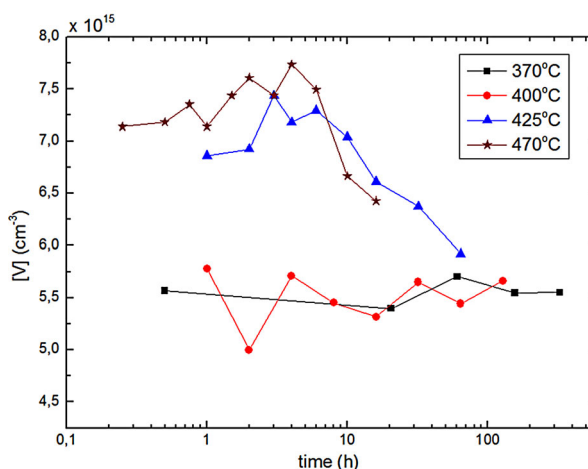
The main reactions used in the simulation are described by $VO_n + O_i \rightarrow VO_{n+1}$ with $n \leq 5$. In addition, we account for the corresponding back reactions of VO and VO_2 whilst no evidence of such reactions is found for VO_3 and VO_4. The sum of the four VO_n species gives information on the evolution of the total vacancy concentration in the system during the different isothermal anneals. This is represented in Fig. 2 where the evolution of the concentration $[V] = [VO] + [VO_2] + [VO_3] + [VO_4]$ is shown for the different temperatures studied. This allows us to find out if other defects play a role in the evolution of the VO_n defects. At 370 and 400 °C, $[V]$ remains constant which indicates that the formation of VO_2, VO_3 and VO_4 arises from VO only and no significant loss of vacancies occurs to other complexes. At higher temperature, the general trend is a slight decrease of $[V]$ with the annealing time, which indicates that VO_4 is not the "final" defect and that larger clusters (VO_n with $n \geq 5$) are formed and/or VO_4 dissociates into other defects. In the present model, we assume that VO_4 is immobile and the reaction $VO_4 + O_i \rightarrow VO_5$ is governed by the diffusion of O_i. However, this reaction is not sufficient to explain the experimental data of VO_4 and also to account for the reduction in the total vacancy concentration, a dissociation term has been added in the simulation model for VO_4 ($VO_4 \rightarrow V + O_4$).

In the simulation, the diffusivity of O_i has been taken from the literature [8]. Diffusivities and dissociation rates of VO, VO_2, and VO_3 have been used as fitting parameters. The initial concentration of VO and O_i were taken from the intensity of their corresponding LVMs, all other defect concentrations were initialized to zero.

Figure 3 shows the evolution of the defect concentrations as measured by FTIR and compared with the simulation results. A good quantitative agreement is obtained between the experimental data and the simulations for VO_n ($n \leq 4$) as well as O_i. In agreement with the literature, VO is highly mobile at these temperatures and reacts rapidly with O_i to form VO_2. The simulation describes very well the decrease of [VO] and the increase of [VO_2]. In particular, at 370 °C,

Original

Paper

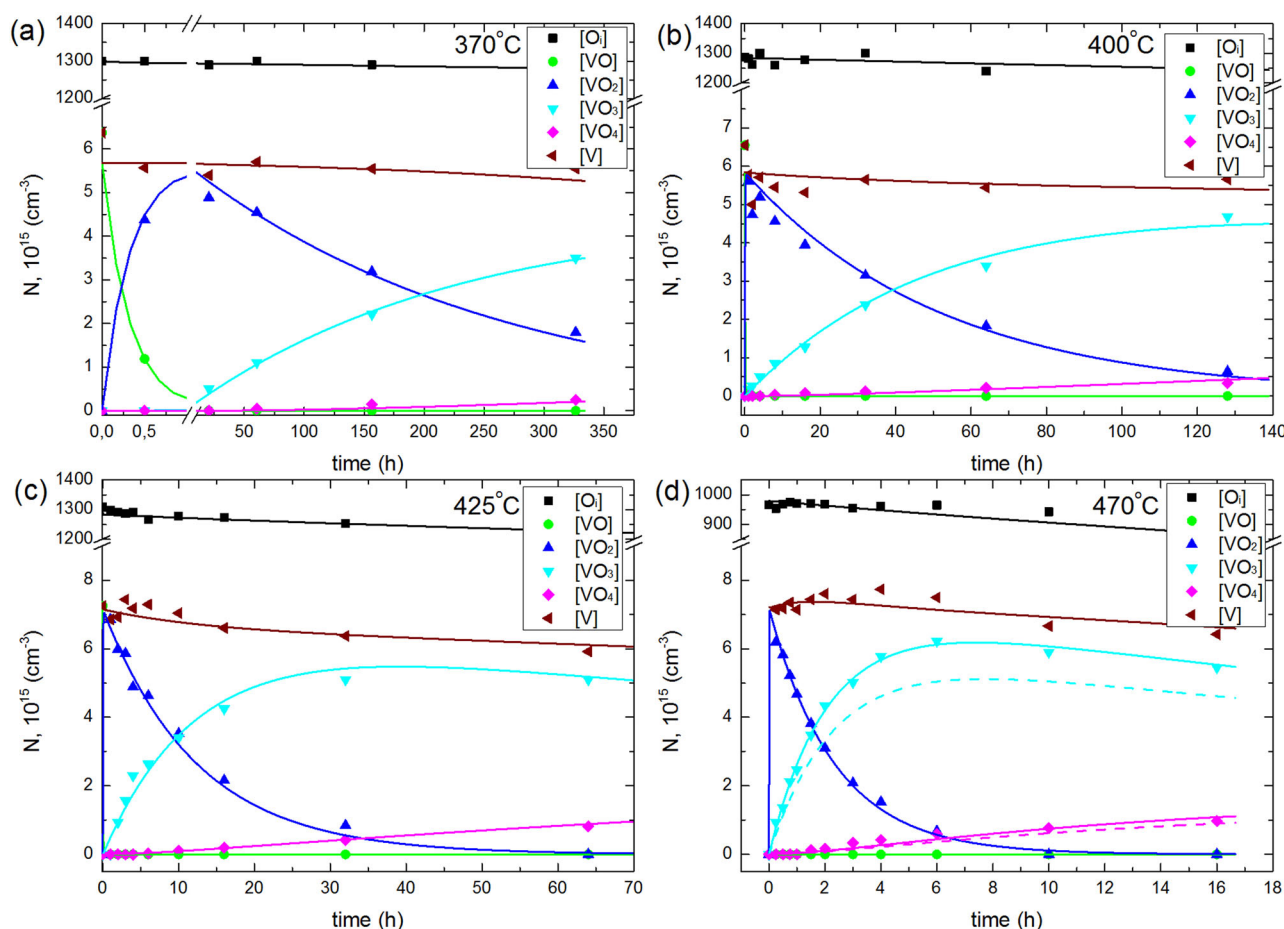Phys. Status Solidi B 251, No. 11 (2014)

2199

Figure 3 Comparison between simulated (line) and experimental concentrations extracted from FTIR (symbols) of O_i and VO_n versus time during isothermal annealing at (a) 370 °C, (b) 400 °C, (c) 425 °C, and (d) 470 °C. The solid lines correspond to the simulation including dissociation of X into VO_3 and the dashed lines in Fig.3d are without dissociation of X.

we are able to reproduce the transformation of VO into VO_2 during the initial annealing stage. At higher temperatures, the transformation occurs rapidly within the first annealing time. After the initial stage and the formation of VO_2, the decrease of $[VO_2]$ is in good correlation with the increase of $[VO_3]$. In the case of VO_3, one can observe a good agreement for the samples annealed at 370, 400, and 425 °C. However, at 470 °C the maximum experimental concentration of VO_3 is not reached by the simulation using only the transformation of VO_2 into VO_3 (see Fig. 3d, dashed lines). In addition, the data in Fig. 2 for the 470 °C sample indicate that $[V]$ slightly increases during the first annealing stages ($\leq$5 h). This may suggest that additional defects contribute somewhat to the formation of the VO_n defects. It is obvious that other defects than VO are formed during the irradiation, including the family of the multi-vacancy–oxygen complexes and also multi-vacancy complexes [16]. These defects can dissociate at high temperature and contribute to, e.g., $[VO]$, $[VO_2]$ and $[VO_3]$. Therefore, in the simulation, we have added a defect X with an initial concentration of about 10% of that of VO. X dissociates at high temperature and forms additional

VO_3 centers. The transformation of VO_3 into VO_4 is then well described by the diffusion of VO_3 to the trap O_i and by the dissociation of VO_4. Moreover, it should be emphasized that X has no effect at 425 °C and below, where the simulations with (solid lines) and without (dashed lines) X are indistinguishable (see Fig. 3a–c).

Figure 4 shows the diffusion and dissociation values deduced from the simulations versus $1/kT$. The values exhibit Arrhenius behavior and the activation energies and prefactors related to the diffusion and the dissociation of the different defects are summarized in Table 1. For instance, the values for VO are in good agreement with values reported previously in the literature [10, 11]. The diffusivity decreases with increasing size of the VO_n complex supporting the assumption that VO_4 is immobile in the studied temperature range. Moreover, the dissociation constant of VO_4 has a prefactor in the range of $10^{12} - 10^{13}$ s^{-1}, which is expected for a dissociative process [17]. The dissociation constant of VO_2 shows relatively low values (both prefactor and activation energy) and further work needs to be pursued to understand this behavior.
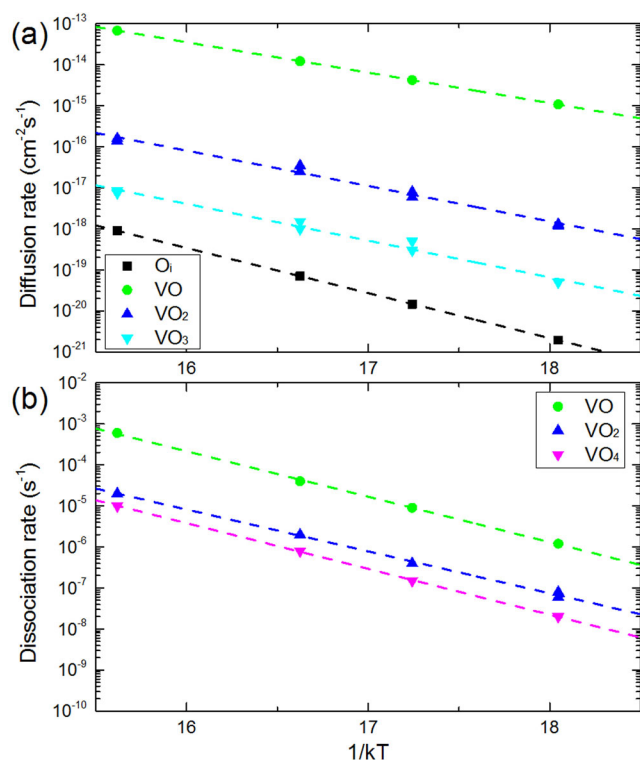
Figure 4 Arrhenius plot of the (a) diffusion and (b) dissociation rates extracted from the simulation.

4 Conclusion Isothermal annealing experiments of VO_n ($n \leq 4$) defects have been carried out using MeV electron irradiated Cz-silicon samples. Simulation results, based

on the theory of diffusion-limited reactions and assuming a sequential build-up of the vacancy–oxygen clusters, show good quantitative agreement with the experimental data. Accordingly, diffusion and dissociation constants have been determined for the VO_n defects and the diffusivity is found to decrease with increasing size of the complex. Further, evidence is obtained for dissociation of VO_4 with the release of vacancies ($VO_4 \rightarrow V + O_4$).

Table 1 Activation energies and prefactors of diffusion and dissociation constants extracted from their corresponding Arrhenius plots.

diffusion constants

defects	E_a (eV)	d_0 (cm^{-2}s^{-1})
O_i	2.53 ± 0.01	0.125 ± 0.005
VO	1.71 ± 0.01	0.026 ± 0.001
VO_2	1.99 ± 0.03	0.005 ± 0.008
VO_3	2.04 ± 0.04	0.001 ± 0.002

dissociation constants

defects	E_a (eV)	k_0 (s^{-1})
VO	2.54 ± 0.04	$(1.2 \pm 0.8) \times 10^{14}$
VO_2	2.38 ± 0.04	$(3.0 \pm 1.2) \times 10^{11}$
VO_4	2.57 ± 0.02	$(2.6 \pm 0.7) \times 10^{12}$

References

[1] K. Bothe and J. Schmidt, J. Appl. Phys. **99**, 013701 (2006).
[2] J. W. Corbett, G. D. Watkins, and R. S. McDonald, Phys. Rev. **135**, A1381 (1964).
[3] J. L. Lindström and B. G. Svensson, Mater. Res. Soc. Symp. Proc. **59**, 45 (1986).
[4] C. A. Londos, L. G. Fytros, and G. J. Georgiou, Defect Diffus. Forum **171–172**, 1–32 (1999).
[5] V. V. Voronkov and R. Falster, J. Electrochem. Soc. **149**(3), G167–G174 (2002).
[6] D. Åberg, B. G. Svensson, T. Hallberg, and J. L. Lindström, Phys. Rev. B **58**, 12944 (1998).
[7] J. L. Lindström, T. Hallberg, J. Hermansson, L. I. Murin, V. P. Markevich, M. Kleverman, and B. G. Svensson, Solid State Phenom. **69–70**, 297 (1999).
[8] R. C. Newman, J. Phys.: Condens. Matter **12**, R335–R365 (2000).
[9] L. I. Murin, T. Hallberg, V. P. Markevich, and J. L. Lindström, Phys. Rev. Lett. **73**, 93–96 (1998).
[10] M. Mikelsen, J. H. Bleka, J. S. Christensen, E. V. Monakhov, B. G. Svensson, J. Harkönen, and B. S. Avset, Phys. Rev. B **75**, 155202 (2007).
[11] V. V. Voronkov, R. Falster, and C. A. Londos, J. Appl. Phys. **111**, 113530 (2012).
[12] J. L. Lindström, L. I. Murin, T. Hallberg, V. P. Markevich, B. G. Svensson, M. Kleverman, and J. Hermansson, Nucl. Instrum. Methods Phys. Res. B **186**, 121–125 (2002).
[13] L. I. Murin, J. L. Lindström, B. G. Svensson, V. P. Markevich, A. R. Peaker, and C. A. Londos, Solid State Phenom. **108–109**, 267–272 (2005).
[14] L. I. Murin and B. G. Svensson, unpublished results.
[15] T. R. Waite, Phys. Rev. **107**, 463–470 (1957).
[16] Y. H. Lee and J. W. Corbett, Phys. Rev. B **13**, 2653–2666 (1976).
[17] J. W. Corbett, in: Electron-Radiation Damage in Semiconductors and Metals, edited by F. Seitz and D. Turnbull (Academic Press, New York, 1966), p. 39.